Residual Stress Influence on Material Properties and Column Behaviour of Stainless Steel SHS

M. Jandera[1], J. Machacek[2]

Faculty of Civil Engineering, Czech Technical University in Prague

Abstract

The paper describes influence of forming-induced residual stresses in stainless steel SHS on both material itself and behaviour of compressed members as well. The residual stress contribution to the stress-strain diagram concerning initial modulus of elasticity and non-linearity is shown by comparison of as-delivered and stress-relieved material. Analytical model covering the influence was developed and verified numerically. FE study using Abaqus software is presented to determine the influence of residual stresses in compressed members both on local and global buckling. Finally, the study includes influence of varying degree of material non-linearity as an independent parameter representing behaviour of various steels in long and stub columns with residual stresses.

Keywords

stainless steel, square hollow section, residual stress, cold forming

1 Introduction

Stainless steels became a competitive structural material while stainless steel members are often represented by cold-formed hollow sections. Many new applications such as oval sections were published [1, 2] recently.

This paper is focused on square hollow sections (SHS) made of austenitic steel Grade 1.4301 which may be regarded as a standard, the most usual one. However, the received results are believed to be valid for all stainless steel grades.

1.1 Residual stress measurement

The forming process of thin-walled structures induces residual stresses which may have a significant effect on structural behaviour.

Residual stresses in cold-formed sections are generally expected to have substantial bending part and comparatively low membrane part, and hereby being the opposite of thermally induced residual stresses in welded or hot-rolled sections (Rasmussen and Hancock [3]). This was also confirmed for residual stresses in stainless steel sections via experimental investigation of members in compression and bending (Rasmussen and Hancock [4, 5]) where large longitudinal bending residual stresses were found.

For carbon SHS the residual stresses were measured by Key & Hancock [6] and a model of their distribution in both directions was proposed.

The first measurements of stresses for whole stainless steel SHS/RHS were published by Young and Lui [7] and Cruise and Gardner [8], where also a distribution of longitudinal bending component was proposed. Measurements embodying new lean duplex stainless steel grade by Huang and Young [9] were published recently.

Later, predictive formulae were published by Jandera and Machacek [10] for both longitudinal (in the direction of member axis) bending ($\sigma_{b,pl}$) and membrane (σ_m) as well as for transverse (in the direction of section webs) bending ($\sigma_{b,pl,t}$) residual stresses. The bending components were assumed considering plastic distribution pattern through thickness. Measurements were made for three webs of two SHS, namely SHS 100x100x3 and 120x120x4.

Especially for the transverse bending, significant simplifications were made and their distribution results from one measurement at the web centre only. The resulting equations for all components are given below:

$$\sigma_m = (-0{,}253+1{,}483(x-x^2))\ \sigma_{0.2} \quad (1)$$

$$\sigma_{b,pl} = (0{,}833+1{,}866(x-x^2))\ \sigma_{0.2} \quad (2)$$

$$\sigma_{b,pl,t} = -0{,}376\ \sigma_{0.2} \quad (3)$$

where x is the relative distance along the web width (with x=0 and x=1 for the edges of the flat web, x=0,5 for the centre of the web) and $\sigma_{0.2}$ is the 0,2 % proof strength of the material at the centre of the web. Plus sign is used for tension and minus for compressive stress. For bending residual stresses the sign is related to the outer surface of the SHS (plus means tension on the outer surface and compression on the inner surface).

Paper Presented by Dr. Michal Jandera - michal.jandera@fsv.cvut.cz

Stresses in the longitudinal direction around cross-section according to (1) and (2) are illustrated in Figs. 1 and 2. This distribution was considered in numerical studies presented hereafter in the paper.

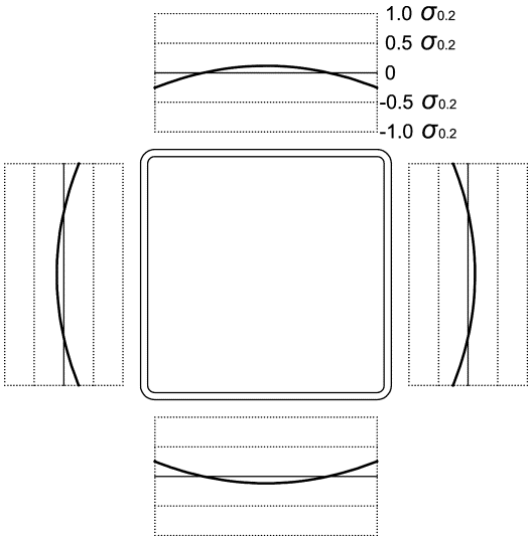

Figure 1 Longitudinal membrane residual stresses σ_m around square hollow section, expression (1)

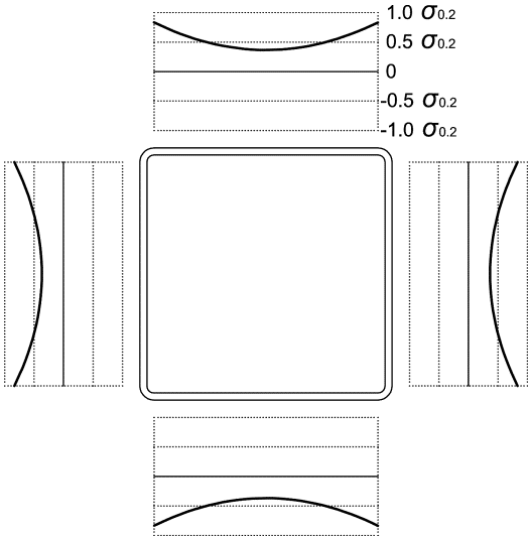

Figure 2. Longitudinal bending residual stresses $\sigma_{b.pl}$ around square hollow section, expression (2).

2 Analytical Model

Together with the FE model described later an analytic model was constituted to study the influence of residual stresses on stress-strain diagram and also to analyse results of the FE model.

2.1 Model description

The analytical model comprised two layers (Fig. 3) through the web thickness. Plastic material response assuming von Mises yielding and Prandtl-Reuss flow rule [11] was considered. The assumptions simplify the true material response of stainless steel behaviour, neglecting e.g. anisotropy, non-symmetry and an increase of ultimate strength due to cold-working. The model was set up in mathematical software Maple.

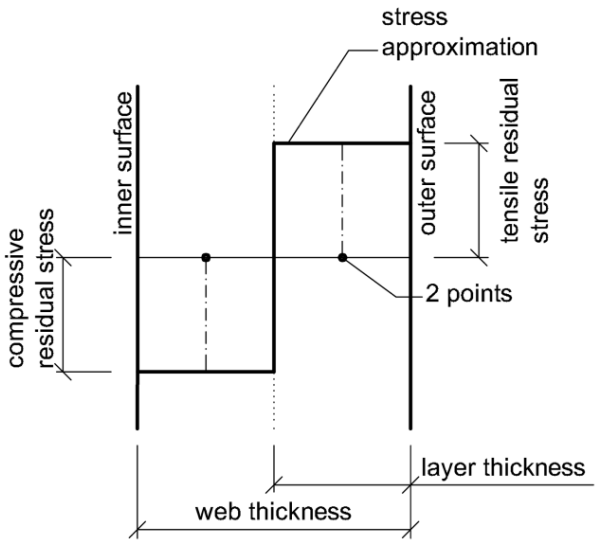

Figure 3 Bending stress approximation considered in the analytical model.

A similar approach was used by Quach et al. [12,13] for prediction of residual stresses due to cold-forming of stainless steel sections or by Rossi et al. [14] for strength enhancement prediction.

2.2 Material properties

The accuracy of the model was studied on tensile tests of coupons taken from two SHS bars (SHS 100x100x3 and SHS 120x120x4), which were previously investigated for residual stresses. For both of them, one specimen was stress-relieved using 650 °C annealing. The material properties were taken from coupons at the web centre and are listed in Tab. 1. The properties define a compound stress-strain diagram developed by Gardner and Nethercot [15] as a modification of Mirambell and Real [16] compound diagram, where:

E_0 is the initial modulus of elasticity,

$\sigma_{0.2}$ the 0.2 % proof strength,

$\sigma_{1.0}$ the 1.0 % proof strength,

σ_u the tensile ultimate strength,

n the Ramberg-Osgood hardening exponent,

$n'_{0.2,1.0}$ the modified Ramberg-Osgood hardening exponent for the second stage of the diagram using $\sigma_{0.2}$ and $\sigma_{1.0}$.

Later this compound diagram was used to study the accuracy of modelling up to the 1 % proof strength.

Table 1 Material properties for flat part of SHS (web centre).Posunout sloupce

Specimen	E_0 [GPa]	$\sigma_{0.2}$ [MPa]	$\sigma_{1.0}$ [MPa]	σ_u [MPa]	n [-]	$n'_{0.2,1.0}$ [-]
100×100×3-F	205.8	417	457	753	7.1	2.3
100×100×3-FA*	211.5	429	456	753	13.4	1.5
120×120×4-F	192.0	429	479	783	4.3	2.7
120×120×4-FA*	205.5	405	441	762	8.1	2.1

* Stress relieved specimen.

Significant difference in the material non-linearity (different Ramberg-Osgood hardening exponent n) and slight change of initial stiffness is obvious by comparison of the as-delivered (F) with stress-relieved specimens (FA). The difference was assigned to the presence of longitudinal bending residual stresses in as–delivered specimens (which were reintroduced by the tensile test).

2.3 Introduction of residual stresses

Together with the comparison of coupon tests the analytical modelling was established. The model was based on stress-relieved material model where longitudinal bending component of residual stresses was employed.

As all the coupons were taken from the web centre, the stress was considered for this part of the section. According to the residual stress measurement, slightly different magnitude was used for SHS 100x100x3 and SHS 120×120×4, respectively. For SHS 100×100×3 the stresses were calculated in (4) and for SHS 120x120x4 in (5) from the 0.2 % proof strength of as-delivered specimens:

$$\sigma_{b.pl} = 0.354 * \sigma_{0.2} = 0.354 * 416.5 = 147.4 \text{ MPa} \quad (4)$$

$$\sigma_{b.pl} = 0.380 * \sigma_{0.2} = 0.380 * 429.0 = 163.0 \text{ MPa} \quad (5)$$

The other components (membrane and transverse bending stresses) should be assumed as zero during the tensile coupon tests. Therefore the longitudinal bending stress component was the only one to be considered. To model the stress-strain behaviour during the tensile coupon test the uniaxial strain increase was considered in the analytical model.

2.4 Model validation

Comparison between the tensile coupon tests and analytical model results is illustrated in Figs. 4 and 5. Considering the model simplifications such as taking perfectly plastic bending residual stress distribution through-thickness and slightly simplified stress-strain behaviour characterised by the compound diagram, the residual stress influence was reasonably approximated. Nevertheless, the prediction is pretty accurate for the initial part, which is essential for buckling of compressed members. The numerical correctness of the analytical model was also confirmed by a FE model of coupon tests.

2.5 Results

The analytical model results confirm that the initial modulus of elasticity and material nonlinearity strongly depends on the residual stress magnitude. Therefore, the material non-linearity is different even for sections of similar magnitude of cold-forming but different residual stresses, i.e. hollow or opened sections. This can also be observed in comparison of Ramberg-Osgood hardening exponent *n* estimated for corner and flat part of the cross-section.

The coefficient *n* for flat parts was in average about 18 % lower (which means larger non-linearity) than for corners in measurements of six SHS tested by Jandera et.al. [17]. As proved e.g. in [8], the corner area is more cold-formed but with significantly smaller residual stresses.

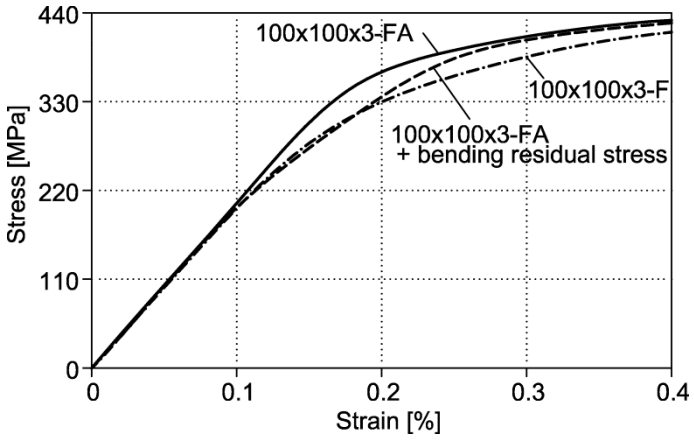

Figure 4 SHS 100×100×3 specimen: as-delivered (F), stress-relieved (FA) and stress-strain curve where longitudinal bending stresses were introduced by the analytical model.

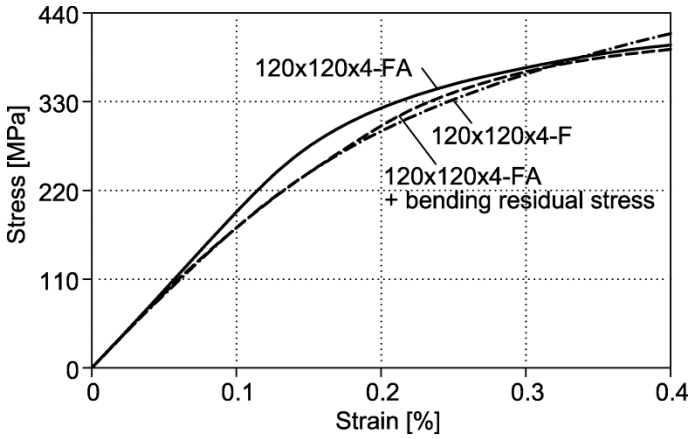

Figure 5 SHS 120×120×4 specimen: as-delivered (F), stress-relieved (FA) and stress-strain curve where longitudinal bending stresses were introduced by the analytical model.

The above presented results imply suitability of the previously mentioned simplification of the residual stress distribution which was also used in the following FE study.

The other purpose of the model was to estimate a residual stress free material behaviour when only coupons for as-delivered sections are tested. As the residual stresses were known, the residual stress free material characteristics were calculated iteratively. Due to the iterative calculation procedure the analytical model was found to be more time-efficient than a FE model of the coupon (which, of course, may also be used for the analysis).

3 FE Model

The proposed model of residual stress distribution was subsequently introduced into a FE model, which was successfully validated in [17] (look there for detailed description of the model).

The parametric studies of influence of residual stresses were divided into two parts: one focused on influence of residual stresses on global column buckling where a pinned column was modelled and the other on local web buckling only, which was represented by a stub column model. The boundary conditions are shown in Fig. 6.

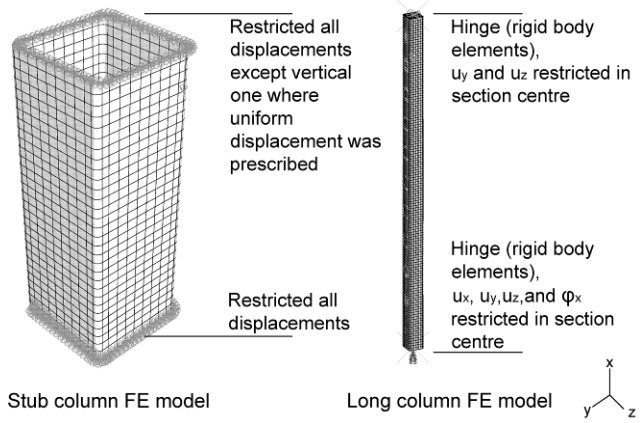

Figure 6 FE models of stub and long column used in the parametric studies.

3.1 Initial geometric imperfections

Local geometric imperfections were considered in the shape of the lowest local buckling mode with the amplitudes measured on the specimens before tests [17]. These web deflections were introduced in models of stub columns as well as long columns. Additionally, global initial geometric column deflections were introduced in the long column model by the lowest global buckling eigenmode with amplitude of $L/2000$, where L is the column length. This value was proposed by Gardner [18] as an average value, lately confirmed by Cruise & Gardner [19].

To study the residual stress influence, the average magnitudes of imperfections were introduced. Using safe (larger) amplitudes of the imperfections would mean smaller residual stress contribution on the load capacity.

3.2 Residual stresses

The bending residual stresses were introduced in 6 integration points with quadratic integration trough the web thickness. The proposed residual stresses pattern was introduced in five modes:

- Membrane: the longitudinal membrane stresses only,
- Longitudinal: the longitudinal membrane and bending stresses,
- Max. longitudinal: the longitudinal membrane and bending stresses, which were taken by the upper bound of the 95% predictive interval (see [10]),
- All: the longitudinal membrane and bending as well as transverse bending stresses,
- Max. all: the longitudinal membrane and bending stresses as well as transverse bending stresses, the longitudinal bending residual stresses were taken as the upper bound of the 95% predictive interval (see [10]).

Bending residual stresses in corners, where no measurement was carried out, were neglected in the analysis. As shown previously by Cruise and Gardner [8], the bending residual stresses in corners are low. This implies, together with increased strength in the corner and comparatively small area of the corner, that their effect on resistance of the whole member is insignificant.

Longitudinal membrane residual stresses in corners were always calculated from condition of equilibrium over the all cross-section. Their magnitudes were very low. This corresponds with conclusions presented by Cruise and Gardner [8] or in the patterns proposed by Key and Hancock [4] for carbon steel SHS.

4 Parametric Study Based on SHS 120x120x4

The study was based on sections SHS 120x120x4 tested at the Czech Technical University in Prague. All principal geometrical and material characteristics were measured. The material characteristics for the corner were taken as measured. For flat parts, the influence of bending residual stress component was removed via the analytical model. The resulting stress-strain diagram therefore corresponded to the stress-relieved material relationship. The modelled corner area was assumed as sum of the own corner area extended for flat web parts considered as twice the web thickness (proposed for SHS by Gardner [18]).

4.1 Influence of residual stresses on global buckling

By analysing column models of varying length, the influence of bending and membrane residual stresses on global buckling capacity over a range of slenderness was assessed. The results of the study are presented in Fig. 7.

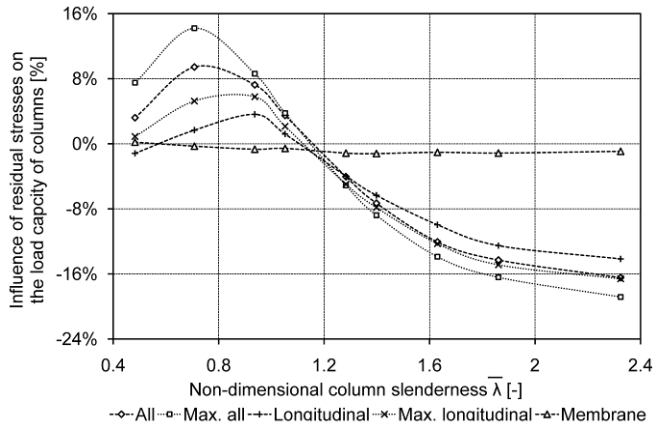

Figure 7 Parametric study of residual stress influence on long column load-carrying capacity.

For non-dimensional slenderness (defined as the square root of the ratio between yield load and elastic buckling load) up to 1.3, the residual stresses may be seen to have a positive influence on load-carrying capacity. Beyond this slenderness, a negative influence is evident. Over the investigated range of slenderness, inclusion of residual stresses causes a variation in resistance between -16 % and +10 % and -20 % to + 14 % if the upper bound of the 95 % predictive interval for the longitudinal bending residual stresses is considered.

The influence of membrane residual stresses was negligible for the whole employed slenderness range.

The variation of resistance results principally from the effect of the bending residual stresses on the non-linearity of the stress-strain curve. A positive influence of residual stresses arises when column failure strains coincide with a region of

increased tangent modulus. This is illustrated for longitudinal bending residual stresses in Fig. 8 where the material response with and without longitudinal bending residual stresses is depicted (the average magnitude of residual stresses for the web was employed). The material stress-strain curve containing residual stresses may be seen to be consistently below the residual stress free curve (i.e. the secant modulus is always lower). However, this is not valid for the tangent modulus, which is known to be fundamental in controlling column buckling resistance. Below approximately 0.12 % strain, the tangent modulus of the stress free curve is higher than that of the residual stresses containing curve. Conversely, for higher strains, the reverse is true.

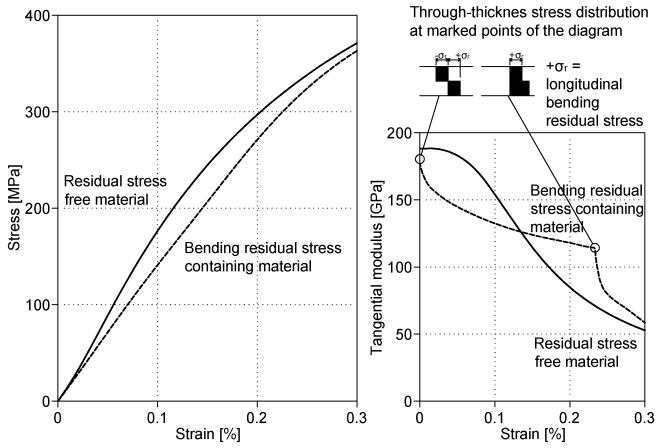

Figure 8. Stress-strain relationship (left) and tangent modulus (right) of material with and without longitudinal bending residual stresses valid for the average web value of SHS 120x120x4.

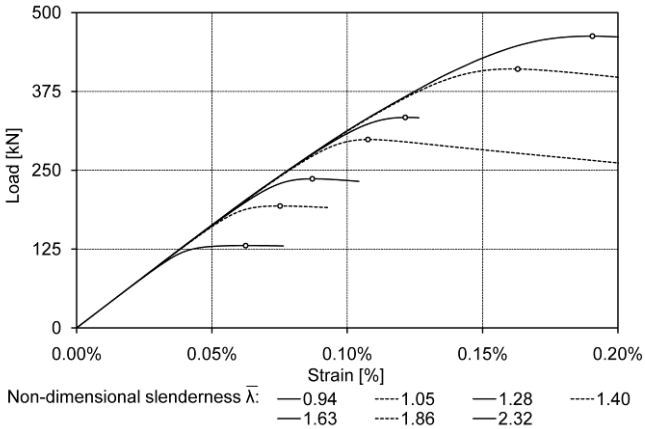

Figure 9 Load-strain diagrams of long columns

From Fig. 9, where load-strain curves of columns are printed (strain denotes ratio of the axial deformation to the column length; similarly in Fig. 11), follows that the failure strains of columns of slendernesses up to 1.3 reach more than 0.12 %. That's the range, where the longitudinal bending residual stresses were found to have positive influence on the tangential modulus.

For higher column slenderness (> 1.3), lower strains are reached at ultimate load. Therefore the tangent modulus for the material where bending residual stresses were included is lower than the tangent modulus of material without residual stresses (Fig. 8), and thus longitudinal bending residual stresses were found to lead to a reduction in load-carrying capacity.

The magnitude of residual stresses clearly influences the variation in load-carrying capacity. It was found that taking mean longitudinal bending residual stress values rather than the upper bound of the predictive interval, sensitivity of the column response was nearly halved for the most sensitive slenderness range. For the large slenderness, the difference was lower.

The transverse bending residual stress was found to emphasize the effect of the longitudinal one and having also significant effect.

4.2 Influence of residual stresses on local buckling

The influence of residual stresses on local buckling capacity was assessed in a similar manner to the above studied global buckling. Stub column models of varying local web slenderness with and without residual stresses were examined. The results are shown in Figure 10. The maximum influence of residual stresses in terms of load-carrying capacity was 9 % and 11 % if the upper bound of the 95% predictive interval for the longitudinal bending residual stresses was considered. Although slightly less sensitive influence than in the column buckling results, similar conclusions can be drawn. The influence of membrane residual stresses was also found to be insignificant in comparison to the influence of the bending components.

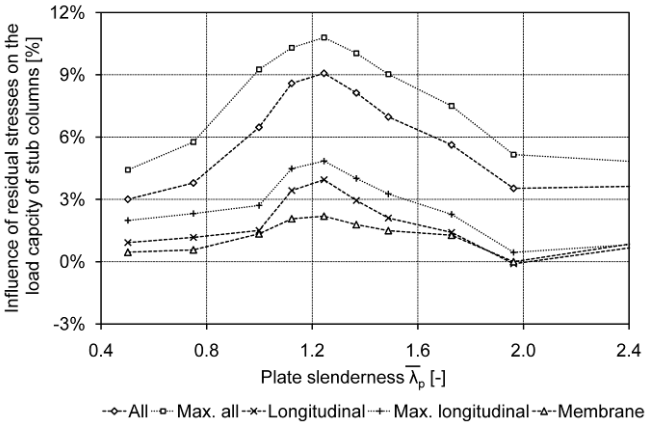

Figure 10 Parametric study of residual stress influence on stub column load-carrying capacity

However, the main difference is that for the local buckling, no negative influence of residual stresses occurred. This is due to the post-buckling behaviour which increases the failure strain for very slender webs. Opposite to post-buckling behaviour of columns, the local buckling failure strain was always greater than 0.12 % (Fig. 11), where residual stresses have the positive influence on tangential modulus.

The highest effect of bending residual stresses was observed for the middle slenderness ($\bar{\lambda}_p$ = 1.0 to 1.3) where the sensitivity of columns is large and the difference of the tangential modulus at failure strain between material with and without bending stresses is the highest.

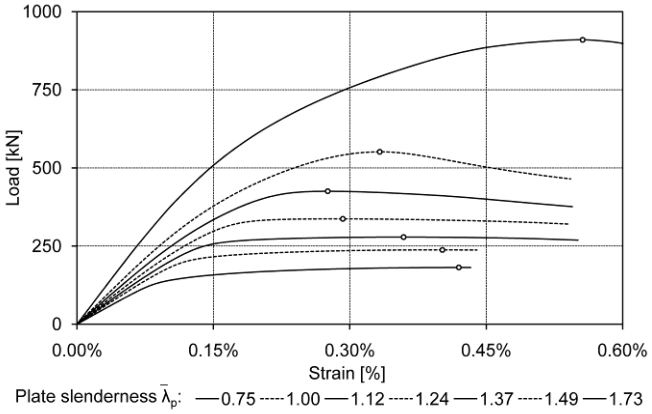

Figure 12 Load-strain diagrams of stub columns.

5 Parametric study on Influence of Ramberg-Osgood Hardening Exponent

The second parametric study was performed in order to explain the influence of residual stresses in materials of various nonlinearities. For the simplicity, in all models only the one-stage Ramberg-Osgood diagram (6) was used for the whole area of cross-section:

$$\varepsilon = \frac{\sigma}{E_0} + 0.002\left(\frac{\sigma}{\sigma_{0.2}}\right)^n \qquad (6)$$

where ε is strain and σ stress. The 0.2 % proof strength was taken according to Eurocode 1993-1-4, i.e. $\sigma_{0.2}$ = 230 MPa for Grade 1.4301. The hardening exponents n was taken as:

- n = 4, representing cold-formed austenitic steels,
- n = 6, representing annealed austenitic steels,
- n = 16, representing the lowest nonlinearity of stainless steels,
- $n = \infty$, bilinear stress-strain diagram representing common carbon steels.

The initial geometric imperfections and residual stresses were employed as above.

5.1 Residual stresses vs material nonlinearity in global buckling

The parametric study was carried out for column slenderness range from 0.8 to 1.8, but results of two the most representative slendernesses $\overline{\lambda}$ = 1.0 and 1.8 only are shown here (Figs. 12 and 13).

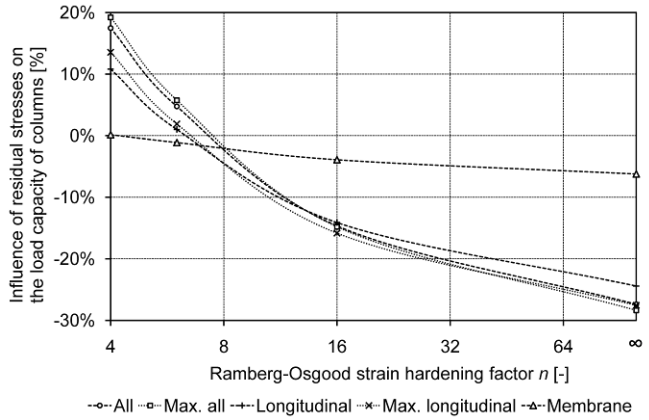

Figure 12 Influence of residual stresses on load-carrying capacity of long column with $\overline{\lambda}$ = 1.0 according to Ramberg-Osgood factor *n*.

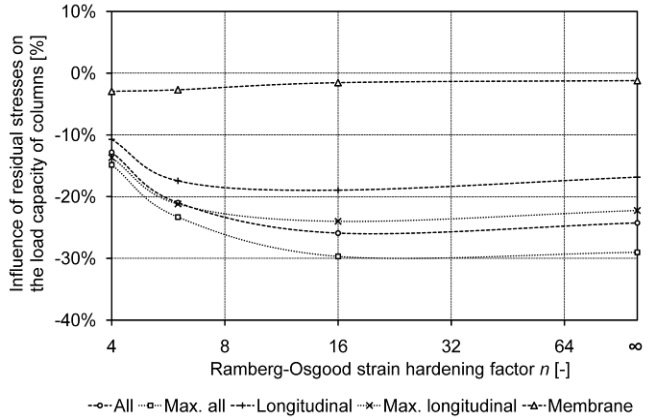

Figure 13 Influence of residual stresses on load-carrying capacity of long column with $\overline{\lambda}$ = 1.8 according to Ramberg-Osgood factor *n*

The results indicate that the residual stresses for the nonlinear material (n = 4 to 6) may increase the load-carrying capacity for the middle slenderness ($\overline{\lambda}$ = 1.0) but for high slenderness ($\overline{\lambda}$ = 1.8) the opposite is true.

For materials with lower nonlinearity of stress-strain diagram, especially for the bilinear stress-strain diagram (e.g. carbon steel), the inclusion of residual stresses cause always decrease in the load capacity as generally known and numerically confirmed for SHS by Key and Hancock [6]. This fact is due to a significant drop in stiffness of materials

which offers none or low strain hardening beyond yield strength. The influence of membrane component of residual stresses is always low.

The magnitude of the influence of residual stresses is, however, rather overestimated in this study due to the simplification of material characteristics. The increased strength of material in the corner area as well as slightly different stress-strain diagram (better represented by the compound Ramberg-Osgood diagram) would suppress the residual stress influence significantly.

5.2 Residual stresses vs material nonlinearity in local buckling

Second part of the study was focused on local buckling and showed similar results (for $\overline{\lambda}_p$ = 1.0 and 1.8 see Figs. 14 and 15).

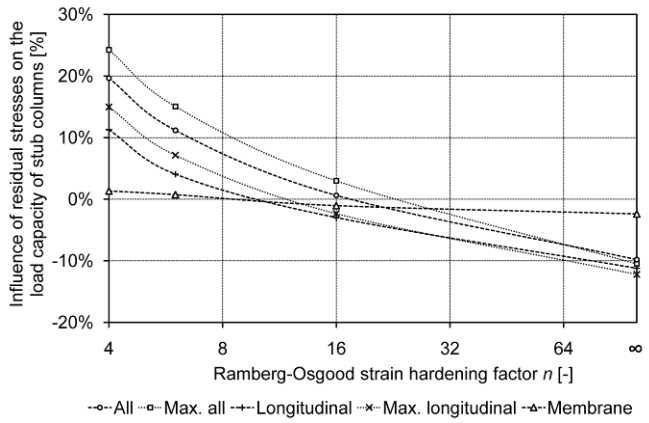

Figure 14 Influence of residual stresses on load-carrying capacity of stub column with $\overline{\lambda}_p$ = 1.0 according to Ramberg-Osgood factor *n*

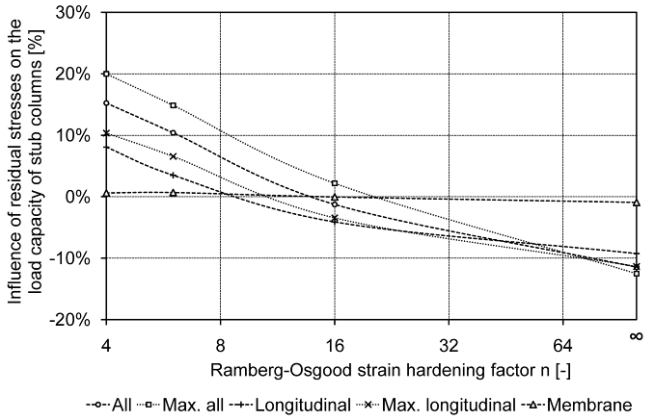

Figure 16 Influence of residual stresses on load-carrying capacity of stub column with $\overline{\lambda}_p$ = 1,8 according to Ramberg-Osgood factor *n*

As in the previous study based on real material characteristics, for nonlinear stress-strain relationships the effect of residual stresses is always positive, whereas for the bilinear material diagram always negative. The influence of membrane residual stresses was negligible in all cases.

6 Conclusions

Numerical investigation concerning influence of residual stresses on stress-strain relationships and column behaviour of structural stainless steel hollow sections is described. Extensive numerical parametric studies using geometrically and materially non-linear FE analysis were performed dealing with long and stub columns to determine the influence of residual stresses on global and local buckling. The results were verified using former experimental results.

Paradoxically, it was found that inclusion of residual stresses may lead to increase of load-carrying capacity in some cases. This was attributed principally to the influence of the bending residual stresses on the material stress-strain curve. It was found that despite the secant modulus being consistently reduced in the presence of residual stresses, the tangent modulus was increased in some regions of the stress-strain curve. The influence of residual stresses was between +10 % to -16 % for global buckling and up to +9 % for local buckling of SHS members using FE model based on measured material characteristics. The influence of membrane residual stresses in the analyses was usually very low and may be in most cases neglected.

Parametric study with varying Ramberg-Osgood strain hardening factor *n* showed that inclusion of residual stress pattern may lead to an increase of the load-carrying capacity of compressed members having non-linear stress-strain diagram, but always to decrease of capacity for materials with bilinear stress-strain diagram (e.g. for common carbon steel). The results proved, that both the residual stresses (bending component mainly) and degree of non-linearity may have significant influence on the load capacity.

Although the behaviour of stainless steel columns with and without bending residual stresses has been investigated in this study, it should be noted that these stresses are inherently present in the stress-strain behaviour of material extracted from structural sections and, therefore, need not generally be re-introduced into numerical models. However, in the design practice as opposed to research, coupon tests are usually not performed and generalized stress-strain relationship is used. In such case the residual stresses are not considered. As shown by the analytical model, the non-linearity is increased significantly by bending residual stress inclusion, accompanied by slight decrease of the initial modulus of elasticity. It is therefore proposed to estimate and use a different (smaller) hardening exponent *n* for cross-sections in which large bending residual stresses are present (notably SHS and RHS).

Acknowledgements

The support of the Czech Science Foundation grant P105/12/P307 “Influence of Cold-Forming on Stainless Steel Mechanical Properties” is gratefully acknowledged.

References

[1] Theofanous, M., Chan, T. M., Gardner, L. Flexural behaviour of stainless steel oval hollow sections. Thin Walled Structures. 2009; 47(6-7), 776 – 787.

[2] Theofanous, M., Chan, T. M., Gardner, L. Structural response of stainless steel oval hollow section compression members. Engineering Structures. 2009; 31(4): 922 – 934.

[3] Rasmussen, K.J.R., Hancock, G.J. Deformations and residual stresses induced in channel section columns by pre-setting and welding. Journal of Constructional Steel Research. 1988; 11(3), 175–204.

[4] Rasmussen, K.J.R., Hancock, G.J. Design of cold-formed stainless steel tubular members, I: Columns. Journal of Structural Engineering. 1993; 119(8), 2349–2367.

[5] Rasmussen, K.J.R., Hancock, G.J. Design of cold-formed stainless steel tubular members, II: Beams. Journal of Structural Engineering. 1993; 119(8), 2368–2386.

[6] Key PW, Hancock GJ. A theoretical investigation of the column behaviour of cold-formed square hollow sections. Thin-Walled Structures 1993; 16(1-4), 31-64.

[7] Young B, Lui WM. Behaviour of cold-formed high strength stainless steel sections, Journal of Structural Engineering 2005;131(11), 1738-45.

[8] Cruise, R.B., Gardner, L. Residual stress analysis of structural stainless steel sections. Journal of Constructional Steel Research. 2008; 64(3), 352 – 366.

[9] Huang Y., Young B. Material properties of cold-formed lean duplex stainless steel sections. Thin-Walled Structures. 2012; 54, 72-81.

[10] Jandera, M., Machacek, J. Measurement of residual stress pattern in stainless steel cold-rolled SHS. In: Proc. 6th International Conference on Thin-Walled Structures, Timisoara. 2011, 619-624.

[11] Hill, R. The Mathematical Theory of Plasticity. Oxford University Press; 1998.

[12] Quach, W.M., Teng, J.G., Chung, K.F. Residual stresses in press-braked stainless steel sections, I: Coiling and uncoiling of sheets. Journal of Constructional Steel Research. 2009; 68(8-9), 1803 – 1815.

[13] Quach, W.M., Teng, J.G. Chung, K.F. Residual stresses in press-braked stainless steel sections, II: Press-braking operations. Journal of Constructional Steel Research. 2009; 68(8-9), 1816 – 1826.

[14] Rossi, B., Degée, H., Pascon, F. Enhanced mechanical properties after cold process of fabrication of non-linear metallic profiles. Thin-Walled Structures. 2009; 47(12), 1575 – 1589.

[15] Gardner, L. Nethercot, D.A. Experiments on stainless steel hollow sections - Part 1: Material and cross-sectional behaviour. Journal of Constructional Steel Research. 2004; 60(9), 1291 – 1318.

[16] Mirambell, E., Real, E. On the calculation of deflections in structural stainless steel beams. Journal of Constructional Steel Research. 2000; 54(1), 109 – 133.

[17] Jandera, M., Gardner, L., Machacek, J. Residual stresses in cold rolled stainless steel hollow sections. Journal of Constructional Steel Research. 2008; 64(11), 1255–1263.

[18] Gardner L. A new approach to structural stainless steel design. Ph.D. thesis. Department of Civil and Environmental Engineering, Imperial College London. 2002.

[19] Cruise R.B., Gardner L. Measurement and prediction of geometric imperfections in structural stainless steel members. Structural Engineering and Mechanics. 2006; 24(1), 63-89

